Pre-print for publication in the IEEE Transactions on Smart Grid, 2015

Data-Driven Thermal Modeling of Residential Service Transformers

Andrew Seier, *Student Member, IEEE,* Paul Hines, *Senior Member, IEEE,* and Jeff Frolik, *Senior Member IEEE*

***Abstract*—Sales of privately-owned, plug-in electric vehicles (PEVs) are projected to increase dramatically in coming years and their charging will impact residential service transformer loads. Transformer life expectancy is related to the cumulative effects of internal winding temperatures, which are a function of loading. Thermal models exist (e.g., IEEE C57.91) for predicting these internal temperatures, the most sophisticated being the Annex G model. While this model has been validated with measurements from large power transformers, small residential service transformers have been given less attention. Given increasing PEV loads, a better understanding of service transformer aging could be useful in replacement planning processes. Empirical data from this work indicate that the Annex G model over-estimates internal temperatures in small, $25\,\mathrm{kVA}$, $65\,^{\circ}\mathrm{C}$ rise, mineral-oil-immersed transformers. This paper presents an alternative model to Annex G by using a genetic program (GP). This model is both simpler and more accurate at tracking empirical transformer data. These results suggest that one can use a simple thermal model in combination with data from advanced metering infrastructure (AMI) to more accurately estimate service transformer lifetimes, and thus better plan for transformer replacement.**

***Index Terms*—Smart grids, power transformers, genetic programming, asset management, electric vehicles.**

I. Introduction

THIS paper focuses on methods used to estimate the lifetime of service transformers in residential areas. The term *service transformer* is used here to define the pole- or pad-mounted transformers that directly serve residential loads. The service transformers considered in this paper are $25\,\mathrm{kVA}$, $65\,^{\circ}\mathrm{C}$ rise mineral-oil-immersed devices. Though these particular assets are fairly inexpensive–around $700 for pole-mounted and $1,500 for pad-mounted plus installation costs–the entirety of the fleet will typically constitute a significant fraction of a distribution utility's physical assets.

Sales of plug-in electric vehicles (PEVs) are expected to greatly increase. Inflating adoption rates are predicted to stress the grid and require distribution transformer replacement [1], [2], [3]. For instance, Level 2 charging of PEVs draws $7.2\,\mathrm{kVA}$ of power from the grid. For a $25\,\mathrm{kVA}$ service transformer, this amounts to 29% of the rated load. The average American household has two vehicles [4]. Given that a single service transformer may serve ten houses, PEV penetration rates of 25% could load a $25\,\mathrm{kVA}$ device to 144% of rated load, if the vehicles charge simultaneously. Because charge times for PEVs are expected to overlap, even low penetrations of PEVs can create harmful overloading for service transformers [5].

Power transformers, such as those serving multiple neighborhoods and rated upwards of $500\,\mathrm{kVA}$, are typically monitored closely as their failure in the grid can be costly to utilities and can cause prolonged outages [6]. However, the cost of monitoring each service transformer on the network is generally too expensive, computationally or monetarily, and approximations are used to determine device lifetimes. However, a utility that has advanced metering infrastructure (AMI) has access to accurate loading history for its service transformers and can estimate wear based upon these data. The expense of tracking these assets are then mostly computational.

Where loading is known for a transformer, artificial neural networks (ANN) have been proposed to match the loading profile of a new transformer to the loading profiles of transformers in a recorded database to yield an estimate of remaining lifetime of the new device [7]. Because this paper looks at the damage caused by new PEV charging loads, representative databases are likely not available. Also, ANNs do not give the utility an intuitive understanding of how they predict their outcomes. Another approach is to probabilistically estimate the number of transformers that will require replacement as a function of predicted PEV adoption rates as discussed in [2]. While this analysis is helpful to utilities, it only helps for budgeting, leaving the real-time health of specific transformers in question. Finally, a thermal model can be used which can yield the desired estimates on transformer life while preserving the connection between how the model works and our intuition about how aging occurs in transformers. Such models can be found in [8].

In general, loading transformers causes heating in the internal windings and degrades the insulating material. The effect of overloading is to cause accelerated aging compared to a unit that is loaded to its rated power. If enough overloading accumulates in a single transformer, its lifetime can be significantly curtailed. Transformer aging theory and modeling methods are discussed in the IEEE Guide to Loading Mineral-Oil Immersed Transformers [8]. Due to the internal heating's exponential dependence on transformer loading, energy-equivalent load profiles without peaks are more economic than those with peaks as seen in (1).

This equation set says that if internal heating is an exponential function of load, $L(t)^x$ with $x > 1$, then the least heat would be created by a *flat* loading profile, K. Because simultaneously charging PEVs from a single service transformer causes large loading peaks, (1) is of importance.

This work was supported in part by the US Dept. of Transportation, through the Univ. of Vermont Transportation Research Center (Grant TRC039) and Green Mountain Power.

A. Seier, P. Hines, and J. Frolik are with the School of Engineering at the University of Vermont, Burlington VT, 05405, USA. Email: aseier@uvm.edu, paul.hines@uvm.edu, jfrolik@uvm.edu.

$$\text{Let} \quad \int_0^T L(t)dt = TK \ , \ L(t) > 0$$
$$\text{Assume} \quad L(t_1) > K \ , \ t_1 \in [0, T]$$
$$\therefore \quad \int_0^T L(t)^x dt > TK^x \ , \ x > 1 \tag{1}$$

Moreover, since aging depends on heating, (1) informs us that an accurate estimation of transformer aging starts with a detailed history of transformer loading. If the loading history is known, two models are given by the IEEE loading guide, Clause 7 and Annex G, for calculating transformer aging [8]. The latter model is more complicated, but it is more accurate. Other methods exist which use a circuit model to depict device heating [9], or attempt a complete 3-D dynamic model [10].

In summary, the use of a thermal model would allow utilities to more closely track their service transformer fleets. Ideally, the model would be concise, intuitive, and accurate so that utilities could track many service transformers with minimal effort. To this end, we propose that there exists a simple thermal model that would track the existing data at least as well as the more complicated Annex G and will better represent heating in service transformers. This model will allow for a computationally inexpensive and accurate description of aging in the service transformer fleet.

This paper is organized as follows, Section II describes the data collection process and devices used. Section III explains present drawbacks to using the IEEE Annex G model and discusses some motivation for using a genetic program (GP) to find a thermal model for service transformers. Section IV details the modeling process via an example with data created with the Annex G model. Section V explains why this modeling process would be of use to utilities. Finally, Section VI summarizes the findings of this work.

II. Data Collection

This paper uses experimental data to validate thermal models for service transformer heating. The following section presents information on how these data were acquired.

Howard Industries smart transformers were used to gather thermal and loading data. When powered, the smart transformers output information about the state of operation of the machine each minute. The key output parameters from the instrumented transformer and accompanying sensors are ambient temperature, internal temperatures, and load. Transformers were installed in two locations in South Burlington, Vermont. The locations of these transformers were chosen to be in areas where loading was expected to peak above the transformer's load rating. Each transformer serves a minimum of eleven homes.

Internal temperature data include the outer low voltage winding (OLVW) temperature which is used in this paper. This reading can be compared with the TW or TO values from the Annex G model, the winding or top oil temperature, respectively. The locations of the temperature probes are shown pictorially in Figure 1.

The data loggers used in this research were Campbell Scientific CR800's which recorded serial output from the smart

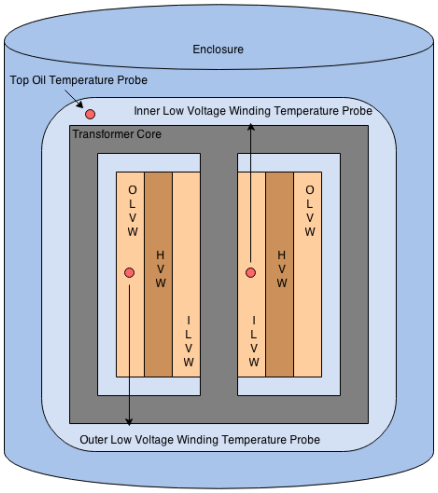

Fig. 1. Transformer winding cross-section. The transformers in this work are 1ϕ. Red circles represent where temperature sensors are located in the Howard Industries devices. Windings show are inner low voltage winding (ILVW), high voltage winding (HVW), and outer low voltage winding (OLVW). The upper-left dot represents the Top Oil (TO) temperature.

transformers as well as output from an ambient temperature sensor. All measurements are real time values which are collected every minute.

Collected data have shown that during periods of high ambient temperature, loading on the instrumented transformers peaked above the rated loading limit. However, the average loading on the transformers was only $9.4\,\mathrm{kVA}$ over the course of three months of logging.

III. Motivation for a New Model

As mentioned in Section I, the IEEE has published models to predict the internal temperature of a transformer. The following Section discusses whether the Annex G model may be overly complicated for modeling $25\,\mathrm{kVA}$ service transformers. It also presents evidence that the predictions of the model may be overly conservative, and thus not an accurate representation of the internal heating of these units.

A. The Annex G Model

For this work, we used the IEEE Annex G model to aid in comparison with previous work [5]. Experimental comparisons for the Annex G model can be found for larger transformers [11]. To our knowledge, there is no existing literature that validates the Annex G model for smaller service transformers.

Using data from a representative day, Figure 2 shows a comparison of top oil temperature data which was output from the Annex G model alongside a measurement of the top oil temperature data from a smart transformer (refer to Figure 1). Figure 2 also shows a comparison of the Annex G model's prediction for the internal hottest spot temperature and the thermal limit for the hottest spot temperature ($110\,^\circ\mathrm{C}$), which when loaded to produces aging at $1\,\mathrm{pu}$ [8]. These data show that during peak loading, the Annex G top oil temperature is overestimating the actual top oil temperature by over $20\,^\circ\mathrm{C}$. Also, even if the Annex G hottest spot estimates

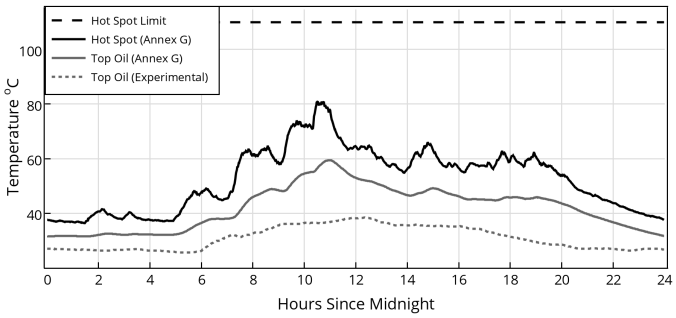

Fig. 2. Comparison of Annex G calculated top oil temperature and measured top oil temperature. From top to bottom, the plot shows the thermal hottest spot temperature limit for normal aging of a transformer ($110\,^{\circ}\mathrm{C}$), the Annex G prediction for hottest spot temperature, the Annex G prediction for top oil temperature, and the measured top oil temperature. All measurements and predictions depend data collected as described in Section II.

are correct in Figure 2, this transformer can be loaded much more before accelerated aging will occur. This is because per unit aging is defined as aging in a transformer with a hottest spot temperature of $110\,^{\circ}\mathrm{C}$, the dashed line at the top of Figure 2.

B. Introduction to Using a Genetic Program

A genetic program (GP) is an evolutionary algorithm (EA) which is used to *evolve* a *population* of *individuals* based on some *fitness* test [12]. The GP does not aim to find the *best solution* given an equation structure, rather the *best structure* given an infinite set of possible structures. Here, a GP is used to create a list of mathematical structures that attempt to model the dynamics of a service transformer's hottest spot temperature. The merits of genetic programming are well documented [12], [13], [14]. A note is in order of preferring an approach that allows for highly complex and disorderly solution structures; a succinct, physically-appropriate solution is ultimately selected by human intervention. The GP will work to continuously output better solutions and it is the job of the user to pick a reasonably intuitive and concise solution. A GP called Eureqa Formulize, developed by Nutonian, is used in this work to find underlying structures in the data. The program is based on the work done in [14].

The solution we will search for in this paper is a single differential equation that reliably models changes in the internal temperature of a service transformer. To see the utility in this, the reader can refer to the Annex G model which is made up of over 30 equations, many of which are differential equations. In contrast, the solution we seek in this paper is of the form shown in (2).

$$\dot{T_{HS}}(s) = f(T_{HS}(s), L(s), T_A(s)) \tag{2}$$

To begin the genetic program, a set of solutions of the form shown in (2) are said to make up the *population* of solutions in the first *generation* of the program. Each solution is termed an *individual*. Note that we use s in (2) to emphasize that the data are discrete.

To assess the *fitness* of each individual in each generation of the GP, the fitness test, $\mathrm{F}(X_{g,i})$, shown in (3) will be used.

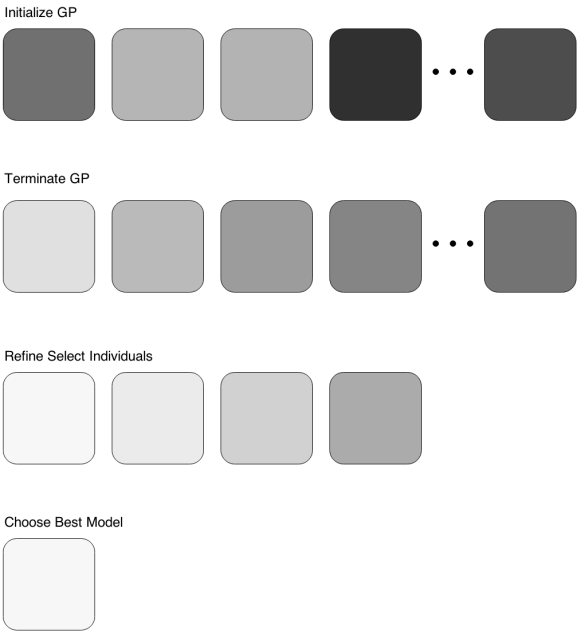

Fig. 3. The model selection process. Each block is an individual solution with the shade representing its absolute fitness, white meaning zero error. The GP is initialized, a set of fit individuals surfaces and the process is terminated, a subset of fit individuals are further refined using a LMS approach, and a single model is ultimately chosen.

The individual, $X_{g,i}$, is number i in the g^{th} generation of the GP. The variables we will use are $L(s)$, $T_A(s)$, and $T_{HS}(s)$ for load, ambient temperature, and hottest spot temperature as a function of the discrete variable s, where S is the number of data points we are using in the GP. Every generation, the N individuals are tested and ranked in descending order of fitness.

$$\mathrm{F}(X_{g,i}) = \frac{1}{S}\sum_{s=0}^{S-1}\left(\dot{T_{HS}}(s) - X_{g,i}\left(L(s), T_A(s), T_{HS}(s)\right)\right)^2 \tag{3}$$

Fit individuals are propagated through future generations as a function of their relative fitness and new individuals are created by combining aspects of fit individuals. In our work, a set of individual solutions are chosen from the final generation. The coefficients on these solutions are then refined via a least mean-squares (LMS) approach, and one solution is ultimately chosen as a best model for the data.

The process is shown graphically in Figure 3. Each block represents an individual in this process (i.e., a solution modeling the change in hottest spot temperature). The shade associated with each individual represents its mean squared error (MSE).

IV. GP Modeling

With regard to the complexity of the Annex G model, the following Section seeks to find a simpler thermal model that tracks internal temperatures as well as the IEEE Annex G model and we detail a broad approach by which a thermal

model can be created to accurately describe the internal heating of service transformers based on user-defined input variables.

To model the dynamics of the Annex G model, we start with a hottest spot temperature profile created by this model. To do this, we input ambient temperature data and actual loading data, which was increased to 150% of the measured values to bring the internal temperatures closer to the transformer's limits and to expose the dynamics of the model. The Annex G hottest spot temperature (T_{HS}), the ambient temperature (T_A), and the loading (L) are used as inputs to the GP. It should be noted that variables T_O and T_W, which are other outputs from the Annex G model, could have been used as additional inputs to the GP. In this way, we would have to actually model *multiple* differential equations, one for each variable, and come up with a set of equations that would need to be integrated forward together to find the hottest spot temperature, T_{HS}. Again, it is our purpose here to simplify, so we choose to relate the input variables to *one* of the original outputs of the Annex G model, the hottest spot temperature.

Heuristically, we would expect that the change in T_{HS} (i.e., $\dot{T_{HS}}$) will depend on the difference between the hottest spot temperature, T_{HS}, and the ambient temperature, T_A. Hence, to simplify the search space, we define T_D as shown in (4), and we seek a differential equation for the change in hottest spot temperature as shown in (5), which is another way of describing (2).

$$T_D = T_{HS} - T_A \tag{4}$$

$$\dot{T_{HS}} = f(L, T_D) \tag{5}$$

The allowable operations for these input variables were: addition, subtraction, multiplication, and negation. This search space has *closure*, meaning that solutions may be composed of results from other solutions, and it is also reasonable to assume that it is *sufficient*, meaning that the input variables and operations are enough to describe the dynamics. The justification of sufficiency comes with the acceptance of a model at the end of this Section.

A. Running the Genetic Program and Selecting Solutions

To acquire our candidate thermal models, we ran the GP for over 6 hours with 16 cloud cores. To reiterate, the GP started with a randomly selected subset of mathematical structures from the infinite solution space created by the assumed variables and mathematical operators of interest. These solutions were then *mutated* and *recombined* by the GP until the GP was manually terminated as discussed in Section III-B. After this, what remains is a population of solutions representing the most fit individuals; the ten simplest out of the final population are considered here. They are shown, ordered by complexity and labeled alphabetically (a-i), in Table I. This table labels each solution equation structure with a letter which will be referenced throughout this paper. Detailed explanation and defense of this process is beyond the scope of this work, but is contained in [12].

TABLE I
STRUCTURES ARISING FROM GP AND FOUR SELECTED STRUCTURES TRAINED ON THE DATA IN FIGURE 4.

ID	Structure for $\dot{T_{HS}}$	Model for $\dot{T_{HS}}$ (Trained in Figure 5)
a	α_1	
b	$\alpha_1 L$	
c	$\alpha_1 L + \alpha_2$	
d	$\alpha_1 L + \alpha_2 T_D$	$0.0367L - 0.0188T_D$
e	$\alpha_1 L + \alpha_2 + \alpha_3 T_D$	$0.0469L - 0.262 - 0.0149T_D$
f	$\alpha_1 + \alpha_2 L^2 + \alpha_3 T_D$	$0.178 + 0.00094L^2 - 0.0149T_D$
g	$\alpha_1 L^2 + \alpha_2 + \alpha_3 T_D^2$	$0.00096L^2 - 0.040 - 0.00022T_D^2$
h	$\alpha_1 L + \alpha_2 L^3 + \alpha_3 T_D$	
i	$\alpha_1 L + \alpha_2 L^4 + \alpha_3 T_D$	

As is common with genetic programs, it is up to the user to select a reasonable solution [12], [13], [15]. Solution (a) from Table I is not a good selection because it is constant that doesn't depend on any of the input variables. Models (b) and (c) do not depend on T_D, which is connected to T_A, a known input to the Annex G model. Therefore, we do not choose these either. Models (h) and (i) begin to create complicated polynomial fits from the variable L and are also not chosen.

We continue with solutions (d), (e), (f), and (g), shown in **bold**. It will be shown that one of these models can be considered acceptable when compared to the Annex G model in the following subsections. If this were not the case, the next logical step would be to include more of the models from Table I to see if any of these yield better results. If no models can ultimately be selected by the end of this process, the assumption is that the solution space is not sufficient and more input variables, beyond our chosen L and T_D, need to be added and the GP must be rerun. For reference, the resulting models from the training discussed in the following subsection are shown in Table I.

B. Fitting Selected Structures to Training Data via Least Mean Squares

The next step is to take the structures obtained from running the GP and find a best LMS fit to make the actual models. In making a model, we must train it on certain data and then check its validity on new data. These models are trained on the inputs shown in Figure 4, where the loading profile is an hour long pulse and the temperature profile is a ramp. During research, training the models with fictitious data like the load pulse and temperature ramp was more successful in finding a best fit. The short load pulse and temperature ramp allows us to separate out dynamics due to loading and temperature differentials.

As specified in [8], emergency overloads are intentional overloads that last for only a short duration. Loading guides in this document cite a maximum emergency overload limit of $2\,\mathrm{pu}$, thus though the load pulse shown is fictitious, it is not an unreasonable estimate to a loading scenario. Loading goes from very underloaded, at $0.5\,\mathrm{pu}$ or $12.5\,\mathrm{kVA}$, to overloaded, at $1.5\,\mathrm{pu}$ or $37.5\,\mathrm{kVA}$. The temperature ramp changes from $0\,^\circ\mathrm{C}$ to $40\,^\circ\mathrm{C}$ during an interval in the middle of the day. Such low temperatures help the model train when T_D is large, and high temperatures allow the model to train when T_D is small. In Fahrenheit, the temperatures go from $32\,^\circ\mathrm{F}$ to $104\,^\circ\mathrm{F}$. This

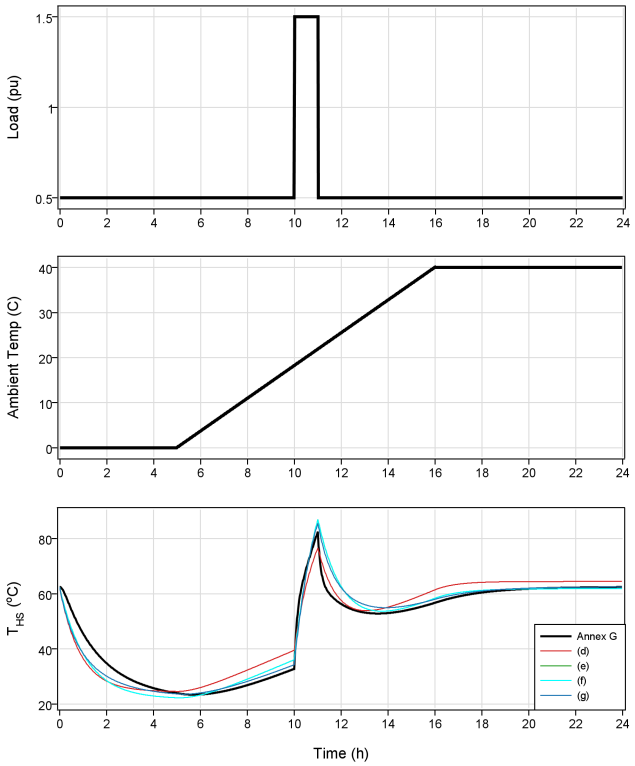

Fig. 4. A T_{HS} curve is produced to train structures (d)-(g). The loading profile (top) and ambient temperature profile (middle) are used to create a the Annex G predicted T_{HS} temperature (bottom-black). Coefficients of structures (d)-(g) are set to minimize differential equation error and then integrated forward and are shown compared to the Annex G prediction (bottom-colors).

ambient temperature spectrum certainly covers the hottest days in a Vermont year, though locals can attest that it does not fully handle the lowest. Again, this training data is meant to have some practical ranges, but need not be experimental for the purposes of training the models.

The Annex G model is then used to predict the hottest spot temperatures throughout the day, shown in Figure 4 (bottom). The models (d)-(g) are then fit to the *change* in the Annex G curve and also shown in Figure 4 (bottom), where they have been integrated forward for comparison of modeled T_{HS} temperatures. Notably, model (d) is the only curve which seems to have a steady state error. Another clarifying point, the models do the *worst* at the beginning of the day when the ambient temperature is low, though all of the models begin with initial conditions from the prior night when ambient temperatures were discontinuously higher as seen in Figure 4 (middle). Abrupt changes like this are included to help train the models by emphasizing the dynamics of the Annex G model, though ambient temperatures do not have such discontinuities in practice. Loading, on the other hand, as expressed in Figure 4 (top) *can* change very rapidly. The LMS fits for the structures obtained from the training portion of this process for the models (d), (e), (f), and (g) are shown in the rightmost column of Table I.

TABLE II
ERROR TABLE: MEAN SQUARED-ERROR (MSE) IN $^{\circ}\mathrm{C}/\mathrm{min}^2$ AND ERROR PER POINT (EPP) IN $^{\circ}\mathrm{C}$ FROM THE TRAINING (T), THE LOW LOAD (L), AND THE HIGH LOAD (H). MODELS REFER TO THOSE IN TABLE I.

ID	MSE T	MSE L	MSE H	EPP T	EPP L	EPP H
d	0.0251	0.0272	0.2311	1.2805	0.4796	-6.0791
e	0.0216	0.0214	0.2011	0.0286	1.8721	3.6869
f	0.0216	0.0272	0.1692	0.0286	-1.0069	-1.0193
g	0.0203	0.0265	0.1580	0.2560	0.3465	-3.4269

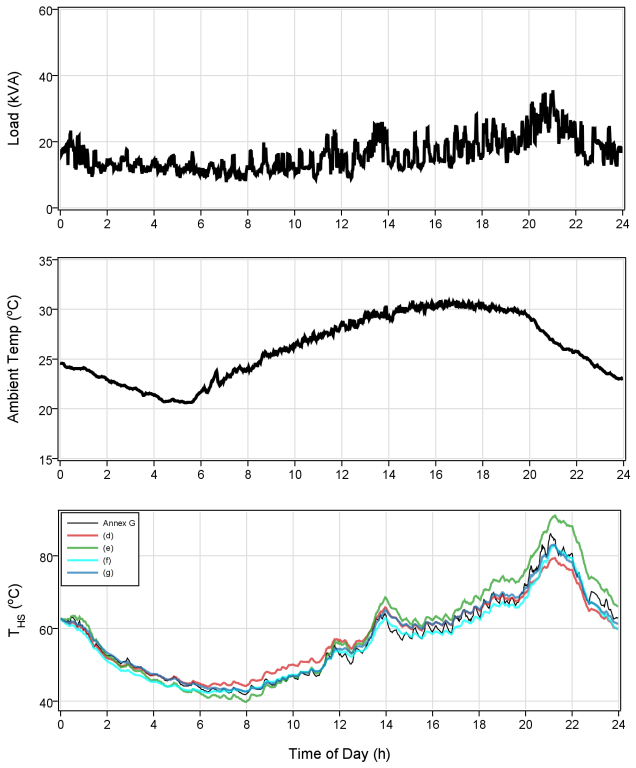

Fig. 5. Model validation via a comparison with independent T_{HS} predictions for low loading. The loading profile (top) and ambient temperature profile (middle) are used to create Annex G and model (d)-(f) T_{HS} predictions (bottom) to validate the models for low loading scenarios.

C. Selecting a Final Model Based on Validation

The four models acquired from the training process are then assessed with new a new load profile, Figure 5 (top), and a new temperature profile, Figure 5 (middle). The loading curve here is measured loading data from one of the smart transformers. This loading is typical of that seen in the experimental neighborhoods where the load breaches the transformer's rated limit only between the hours of 8 PM and 10 PM. The ambient temperature curve shows that this data was collected on a hot day, at least for Vermont.

Figure 5 (bottom) shows the comparison of the resulting forward integrations of models (d), (e), (f), (g). To create these curves, the Annex G method was used to find an estimate for the transformer's hottest spot to which the models are compared. Model (d) is seen to overestimate the Annex G hottest spot temperature between 8 AM and 10 AM and underestimate between the hours of 8 PM and 10 PM. Model (e) is seen to overestimate the Annex G hottest spot temperature between 2 PM and 12 AM the next day and the model does not seem

to converge at the end of the day. Model (f) is arguably the best fit, though model (g) is also very good. Though beyond the scope of this paper, validation runs for these models with different loading levels show that model (f) outperforms all of the other models and thus it was selected from the original structures shown in Table I. A summary of the different model fits is shown in Table II. This table shows the mean squared error (MSE) for each of the models in training (T), low-load validation (L) which is shown in Figure 5, and high-load validation (H) which is not shown. The MSE has units of ${}^{\circ\mathrm{C}}/_{\mathrm{min}}{}^{2}$ because it is relating to the *change* in the hottest spot temperature. Also tabulated are the error per point (EPP) which is a measure of how symmetric the error is. This number is found by summing the errors and dividing by the number of data points and has units of $^{\circ}\mathrm{C}$. Together the MSE and EPP yield a more complete description of the model's ability to track the Annex G predictions. From Table II, model (f) has the most consistently low EPP and has low MSE.

D. Results from Modeling Approach

This process has shown that many models came organically out of a GP. From these models, four were selected for further study that seemed to be both well related to the physics of the actual problem and reasonably simple. The actual coefficients for these models were thrown away so that the structures were kept. They were then re-fitted with with new coefficients using fictional training data and the least mean squares method. To understand whether these fits worked for the specific data or generally for other data sets, the models were validated by integrating them forward with new data. These results show that, qualitatively, all of the models tracked both the changes in temperature of the hottest spot, as predicted by the Annex G method, as well as the overall accumulated hottest spot temperature. We showed that the best model for the Annex G method was (f) as re-stated in (6). The achievement here is finding a differential equation that use only two measurable inputs, three terms, and still tracks the Annex G output reasonably well for very different loading data sets.

$$\dot{T_{HS}} \approx f(L, T_D) = 0.178 + 0.000939L^2 - 0.0149T_D \quad (6)$$

Recall that the Annex G model is made up of a large set of differential equations. Thus, the model presented in (6) manages to follow the dynamics of the Annex G model's predictions of the hottest spot temperature, Figure 5 (bottom), while being much simpler. Model (f) is not meant to be a replacement for the Annex G model for *all* transformers. However, we have conjectured that a $25\,\mathrm{kVA}$ service transformer may not require the full complexity of the Annex G model and have shown that the structure of model (f), using only *one* differential equation, has been validated to predict hottest spot temperatures in accordance with the IEEE standard model. It should be noted that this model has been trained and validated against the Annex G model for a single set of transformer parameters. This means that the model coefficients may need to be tuned for use with slightly different transformers.

It is important to note that the model in (6) makes physical sense, given thermodynamics and circuit theory. If we recall the equivalent circuit for a transformer, there are power losses associated with the modeled resistance of the core and the resistance of the winding. These power losses manifest themselves as heating and are proportional to the square of the current through the resistors. Because the voltage at a transformer is relatively constant, the load (L) served by a transformer is proportional to the current through the windings. The power loss in the winding resistance is then proportional to the square of this instantaneous current. Hence, the L^2 term in (6) supports this rationalization. Furthermore, Newton's Law of Cooling tells us that a body cools in proportion to the difference between its temperature and the ambient temperature, i.e., the term T_D from (6) [16]. Finally, the constant in this equation may be an adjusting factor since we are directly relating an internal temperature to the ambient temperature. Such physical insight would not be obtained using alternative empirically-based modeling methods such as artificial neural networks.

V. Connection to Asset Management

Thus far, we have explained how the Annex G model may not be appropriate for describing the heating measured experimentally in our instrumented service transformers. We have also proposed an approach by which a simple thermal model can be found for service transformers. This Section seeks to explain how a utility would be able to leverage such a model for better asset management of its service transformer fleet.

The large fleet of service transformers owned by utilities is an important subset of assets that must be appropriately managed. Given that the utility in question has already installed AMI, access to loading data for these transformers is relatively inexpensive. This includes getting local ambient temperatures from nearby national weather stations (e.g., the KBTV station for South Burlington). Initial results show that the Annex G thermal model for loading these transformers is overly conservative in that it predicts internal temperatures to be higher than what are experimentally recorded. In addition, the cumbersome nature of the model along with the large number of device-specific constants required, presents a barrier to utilities. The approach to modeling hot-spot temperatures can be used by utilities to find a concise, intuitive model which can leverage loading data.

In this way, utilities see the effect of increased loading from PEV charging as it appears. This requires neither a history of transformer failure as a comparison nor a cumbersome model which is unintuitive and computationally intense. The method only depends on evidence that insulation pyrolysis, the destruction of the material via heating, is the determining factor in transformer aging. With up-to-date information on service transformer aging, utilities can preemptively install additional capacity before certain devices breakdown and appropriately budget for future device purchase and installation.

In addition, the approach explained in this paper is flexible to the input data used. The Annex G model uses only loading and ambient temperature as inputs, though other factors (e.g., wind speed, solar intensity, etc.) may be important in properly

modeling transformer heating. By measuring this data and using it as an input to the approach shown in Section IV, such dependencies can be included. For example, work with ANNs has shown that current harmonics in devices may have an effect on heating which is not captured by the Annex G model [17]. Another factor that may be of import is hydrolysis, which has been shown to effect insulation aging for transformers loaded far below their rated limits [18]. Finally, utilities would also have the option to include load management, and control loading based on calculated internal temperatures. Monitoring their transformer fleet in this way would allow for more accurate and flexible management.

VI. Conclusion

Initial data collected for this paper indicate that the Annex G model is overly conservative in that it overestimates internal temperatures for the instrumented $25\,\mathrm{kVA}$ service transformers used in this work (see Figure 2). Because a precise estimate of a transformer's hottest spot temperature is the standard indicator for insulation aging, an approach to finding a more appropriate model was detailed. The approach used a genetic program to remodel output from the Annex G model to indicate the effectiveness of the method. The result of this approach was shown in (6), which was far simpler than the Annex G model, and tracked the model well. Our existing measurement system did not provide data for hottest spot temperature; collection and modeling of hottest spot data remains for future work.

Given that utilities have increasing access to residential load time-series data and that weather data are readily available, real-time monitoring of service transformers is a realistic goal. If these assets are monitored, utilities can gain information on how much additional loading capacity exists at the residential level to serve predicted PEV charging requirements. They can also closely monitor the aging rates of these devices and make decisions on how to schedule future replacements and upgrade these devices proactively instead of reactively. Therefore, by leveraging data collected by AMI, utilities can more closely monitor aging in assets that were previously difficult to track.

Acknowledgment

This work was supported in part by the US Department of Transportation, through the University of Vermont Transportation Research Center (Grant No. TRC039) and Green Mountain Power.

References

[1] L. Fernández, T. Román, R. Cossent, C. Domingo, and P. Frías, "Assessment of the impact of plug-in electric vehicles on distribution networks," *Power Systems, IEEE Transactions on*, vol. 26, no. 1, pp. 206–213, 2011.

[2] J. Sexauer, K. McBee, and K. Bloch, "Applications of probability model to analyze the effects of electric vehicle chargers on distribution transformers," *Power Systems, IEEE Transactions on*, vol. 28, no. 2, pp. 847–854, May 2013.

[3] Q. Gong, S. Midlam-Mohler, V. Marano, and G. Rizzoni, "Study of PEV charging on residential distribution transformer life," *Smart Grid, IEEE Transactions on*, vol. 3, no. 1, pp. 404–412, 2012.

[4] United States Department of Transportation. Number of households by household driver count. [Online]. Available: http://nhts.ornl.gov/tables09/FatCat.aspx

[5] A. Hilshey, P. Hines, and J. Dowds, "Estimating the acceleration of transformer aging due to electric vehicle charging," in *Power and Energy Society General Meeting, 2011 IEEE*, 2011, pp. 1–9.

[6] M. Pradhan and T. S. Ramu, "On the estimation of elapsed life of oil-immersed power transformers," *Power Delivery, IEEE Transactions on*, vol. 20, no. 3, pp. 1962–1969, July 2005.

[7] J. Jardini, H. Schmidt, C. M. V. Tahan, C. C. B. De Oliveira, and S. U. Ahn, "Distribution transformer loss of life evaluation: a novel approach based on daily load profiles," *Power Delivery, IEEE Transactions on*, vol. 15, no. 1, pp. 361–366, Jan 2000.

[8] "IEEE guide for loading mineral-oil-immersed transformers," *IEEE Std C57.91-1995*, pp. 1–112, 2012.

[9] G. Swift, T. Molinski, and W. Lehn, "A fundamental approach to transformer thermal modeling. I. theory and equivalent circuit," *Power Delivery, IEEE Transactions on*, vol. 16, no. 2, pp. 171–175, 2001.

[10] M. Rosillo, C. Herrera, and G. Jaramillo, "Advanced thermal modeling and experimental performance of oil distribution transformers," *Power Delivery, IEEE Transactions on*, vol. 27, no. 4, pp. 1710–1717, 2012.

[11] D. Susa, M. Lehtonen, and H. Nordman, "Dynamic thermal modelling of power transformers," *Power Delivery, IEEE Transactions on*, vol. 20, no. 1, pp. 197–204, 2005.

[12] J. Koza, *Genetic Programming: On The Programming of Computers by Means of Natural Selection*. MIT Press, 1992.

[13] J. Bongard and H. Lipson, "Automated reverse engineering of nonlinear dynamical systems," *PNAS*, vol. 104, no. 24, pp. 9943–9948, June 2007.

[14] M. Schmidt and H. Lipson, "Distilling free-form natural laws from experimental data," *Science*, vol. 324, no. 5923, pp. 81–85, 2009. [Online]. Available: http://www.sciencemag.org/content/324/5923/81.abstract

[15] H. Kamal and M. Eassa, "Solving curve fitting problems using genetic programming," in *Electrotechnical Conference, 2002. MELECON 2002. 11th Mediterranean*, 2002, pp. 316–321.

[16] L. C. Burmeister, *Convective Heat Transfer*, 2nd ed. Wiley-Interscience, 1993.

[17] J. Pylvanainen, K. Nousiainen, and P. Verho, "Studies to utilize loading guides and ann for oil-immersed distribution transformer condition monitoring," *Power Delivery, IEEE Transactions on*, vol. 22, no. 1, pp. 201–207, Jan 2007.

[18] A. Kachler and I. Hohlein, "Aging of cellulose at transformer service temperatures. part 1: Influence of type of oil and air on the degree of polymerization of pressboard, dissolved gases, and furanic compounds in oil," *Electrical Insulation Magazine, IEEE*, vol. 21, no. 2, pp. 15–21, 2005.

Andrew Seier (S'11) received his B.S.E.E in 2011 and his M.S.E.E. in 2013 from the University of Vermont. His master's thesis was "Thermal Modeling of $25\,\mathrm{kVA}$ Transformers and an Approach to Load Managemnet".

Paul D.H. Hines (S'96, M'07, SM'14) received the Ph.D. in Engineering and Public Policy from Carnegie Mellon University in 2007 and M.S. (2001) and B.S. (1997) degrees in Electrical Engineering from the University of Washington and Seattle Pacific University, respectively. He is currently an Assistant Professor in the School of Engineering, and the Dept. of Computer Science at the University of Vermont.

Jeff Frolik (S'85, M'95, SM'11) received the B.S.E.E. degree from the University of South Alabama in 1986, the M.S.E.E. degree from the University of Southern California in 1988 and the Ph.D. degree in Electrical Engineering Systems from the University of Michigan in 1995. He is an Associate Professor in the School of Engineering at University of Vermont.